

## Three-Component Soliton States in Spinor $F=1$ Bose-Einstein Condensates

T. M. Bersano,<sup>1</sup> V. Gokhroo,<sup>1</sup> M. A. Khamehchi,<sup>1</sup> J. D'Ambroise,<sup>2</sup> D. J. Frantzeskakis,<sup>3</sup>  
P. Engels,<sup>1</sup> and P. G. Kevrekidis<sup>4</sup>

<sup>1</sup>*Washington State University, Department of Physics & Astronomy, Pullman, Washington 99164 USA*

<sup>2</sup>*Department of Mathematics, Computer & Information Science, State University of New York (SUNY) College at Old Westbury, Westbury, New York 11568, USA*

<sup>3</sup>*Department of Physics, National and Kapodistrian University of Athens, Panepistimiopolis, Zografos, Athens 15784, Greece*

<sup>4</sup>*Department of Mathematics and Statistics, University of Massachusetts, Amherst, Massachusetts 01003, USA*



(Received 23 May 2017; revised manuscript received 14 November 2017; published 6 February 2018)

Dilute-gas Bose-Einstein condensates are an exceptionally versatile test bed for the investigation of novel solitonic structures. While matter-wave solitons in one- and two-component systems have been the focus of intense research efforts, an extension to three components has never been attempted in experiments. Here, we experimentally demonstrate the existence of robust dark-bright-bright (DBB) and dark-dark-bright solitons in a multicomponent  $F = 1$  condensate. We observe lifetimes on the order of hundreds of milliseconds for these structures. Our theoretical analysis, based on a multiscale expansion method, shows that small-amplitude solitons of these types obey universal long-short wave resonant interaction models, namely, Yajima-Oikawa systems. Our experimental and analytical findings are corroborated by direct numerical simulations highlighting the persistence of, e.g., the DBB soliton states, as well as their robust oscillations in the trap.

DOI: 10.1103/PhysRevLett.120.063202

Solitons are localized waves propagating undistorted in nonlinear dispersive media. They play a key role in numerous physical contexts [1]. Among the various systems that support solitons, dilute-gas Bose-Einstein condensates (BECs) [2,3] provide a particularly versatile test bed for the investigation of solitonic structures [4–6]. In single-component BECs, solitons have been observed either as robust localized pulses (bright solitons) [7–11] or density dips in a background matter wave (dark solitons) [12–21], typically in BECs with attractive or repulsive interatomic interactions, respectively. Extending such studies to two-component BECs has led to rich additional dynamics. Solitons have been observed in binary mixtures of different states of the same atomic species, so-called pseudospinor BECs [22,23]. In particular, dark-bright (DB) [16,24–27], related SO(2) rotated states in the form of dark-dark solitons [28,29], as well as dark-antidark solitons [30], have experimentally been created in binary  $^{87}\text{Rb}$  BECs. Interestingly, although such BEC mixtures feature repulsive intra- and intercomponent interactions, bright solitons do emerge due to an effective potential well created by the dark soliton through the intercomponent interaction [31]. Such mixed soliton states have been proposed for potential applications. For example, in the context of optics where these structures were pioneered [32,33], the dark soliton component was proposed to act as an adjustable waveguide for weak bright solitons [34]. In multicomponent BECs, compound solitons of the mixed type could also be used for all-matter-wave waveguiding, with the dark soliton

building an effective conduit for the bright one, similar to all-optical waveguiding in optics [35]. Apart from pseudo-spinor BECs, such mixed soliton states have also been predicted to occur in genuinely spinorial BECs, composed of different Zeeman sublevels of the same hyperfine state [36–38]. Indeed, pertinent works [39,40] have studied the existence and dynamics of DB soliton complexes in spinor  $F = 1$  BECs. However, experimental observation of such states has not been reported so far.

Here we report on the systematic experimental generation of three-component DB soliton complexes of the dark-bright-bright (DBB) and dark-dark-bright (DDB) types, in an  $F = 1$  condensate of  $^{87}\text{Rb}$  atoms. While DB solitons normally consist of two atomic states (e.g., two  $F = 1$  Zeeman sublevels or a combination of Zeeman sublevels of  $F = 1$  and  $F = 2$  states of  $^{87}\text{Rb}$  [24–29]), here we use all three Zeeman  $F = 1$  sublevels to generate three-component solitons in an elongated atomic cloud. In our theoretical analysis, we employ a multiscale expansion method to derive such vector soliton solutions of the pertinent Gross-Pitaevskii equations (GPEs). We show that DBB and DDB solitons can be approximated by solutions of Yajima-Oikawa (YO) systems [41–43]. We thus provide a connection with universal long-short wave resonant interaction (LSRI) processes [44,45] which appear in a wide range of contexts, including hydrodynamics [45], plasmas [41,44], condensed matter [42], nonlinear optics [46], negative refractive index media [47], etc. Such a connection allows for an approximate analytical description (based on the YO picture) of  $F = 1$

spinor solitons and yields, in turn, important information on the relevant spatial and temporal scales, where these structures can be observed. It also allows for a systematic study on their dynamics, in terms of direct numerical simulations. Indeed, such simulations (and associated numerical initializations) are used to corroborate our experimental and analytical identification of these solitonic structures.

To begin our discussion of the three-component solitonic structures, we first present examples for their realization in experiments. The three components are given by the three different Zeeman sublevels of the  $F = 1$  state of  $^{87}\text{Rb}$ , and are designated by their magnetic quantum numbers  $|F, m_F\rangle = |1, -1\rangle, |1, 0\rangle$ , and  $|1, +1\rangle$ . The experiments begin with a single-component BEC of approximately  $0.8 \times 10^6$  atoms. The atoms are confined in an elongated harmonic trap with frequencies  $\{\omega_x, \omega_y, \omega_z\} = 2\pi \times \{1.4, 176, 174\}$  Hz, where  $z$  is the vertical direction. The trap is formed by a focused dipole laser beam and is independent of the atomic hyperfine state. A magnetic bias field of 45.5 G is applied along the weakly confining direction. This field leads to a Zeeman splitting of the energy levels. As a consequence, populations can be transferred between the three states by using adiabatic radio frequency (rf) sweeps. Because of the quadratic Zeeman shift, spin-changing collisions are energetically suppressed in the experiment. However, we have also confirmed by means of direct numerical simulations that the results in the theoretical considerations below do not change upon inclusion of small values of the quadratic Zeeman effect [37,48].

To generate DBB solitons such as the ones shown in Fig. 1(a), we begin with all atoms in the  $|1, -1\rangle$  state. A small fraction of atoms is uniformly transferred to the  $|1, 0\rangle$  state using a rf sweep. Subsequently, a weak magnetic gradient is applied along the long axis of the BEC (i.e., the  $x$  axis) for approximately 2–3 sec. Since the states have different magnetic moments, this induces superfluid-superfluid counterflow and leads to the formation of DB solitons; see details of this technique in Refs. [24,28]. In the present experiment, the dark solitons reside in the  $|1, -1\rangle$  state and the bright component is formed by the  $|1, 0\rangle$  state. After the removal of the gradient, a second rf transfer moves a fraction of the atoms from the  $|1, 0\rangle$  state to the  $|1, +1\rangle$  state, forming DBB solitons. After a variable evolution time during which the solitons are kept in the trap, a Stern-Gerlach imaging technique is used to individually image all three components in one single run of the experiment [49]. In many runs, DBB solitons can be observed at times up to several seconds after their creation. Decaying solitons feature an increased filling of their dark notch with atoms of the dark component, while the bright components lose confinement and form diffuse cloudlets; cf. Fig. 1(b).

To theoretically trace the formation of compound soliton structures, we resort to mean-field theory. In this framework,

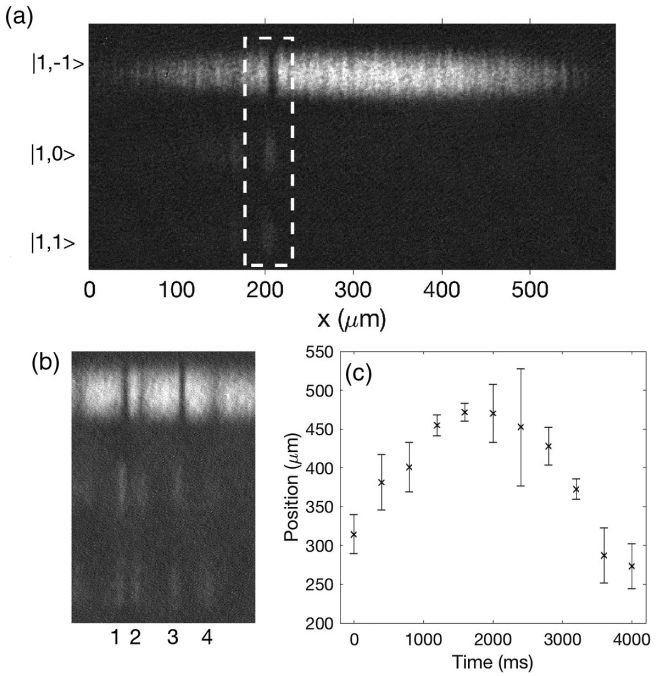


FIG. 1. (a) Experimental time-of-flight (TOF) image of a DBB soliton (boxed). To verify the stability of the soliton, a 100 ms in-trap evolution time was applied after DBB soliton formation. The relative population of the three states  $|1, -1\rangle$ ,  $|1, 0\rangle$ , and  $|1, +1\rangle$  is 97:2:1. (b) At longer times the solitons start to decay. Two stable solitons (1 and 3) are present next to two decaying solitons (2 and 4) after 400 ms of in-trap evolution. (c) Soliton oscillation in the harmonic trap. Six images were taken at each 400 ms interval.

the wave functions  $\psi_{\pm 1,0}(x, t)$  of the three hyperfine components ( $m_F = \pm 1, 0$ ) of a quasi one-dimensional  $F = 1$  spinor BEC obey the following GPEs [39,40,50,51]:

$$i\partial_t\psi_{\pm 1} = \mathcal{L}\psi_{\pm 1} + \lambda_a(|\psi_{\pm 1}|^2 + |\psi_0|^2 - |\psi_{\mp 1}|^2)\psi_{\pm 1} + \lambda_a\psi_0^2\bar{\psi}_{\mp 1}, \quad (1a)$$

$$i\partial_t\psi_0 = \mathcal{L}\psi_0 + \lambda_a(|\psi_1|^2 + |\psi_{-1}|^2)\psi_0 + 2\lambda_a\psi_{-1}\bar{\psi}_0\psi_{+1}, \quad (1b)$$

where  $\mathcal{L} = -\frac{1}{2}\partial_x^2 + V(x) + \lambda_s(|\psi_{-1}|^2 + |\psi_0|^2 + |\psi_1|^2)$  and  $V(x) = (1/2)\Omega^2x^2$ , with  $\Omega = \omega_x/\omega_{\perp}$ . We use  $\omega_x = 1.4$  and  $\omega_{\perp} = 175$  Hz, as per the experimental setup. Finally, the coupling coefficients for “symmetric” spin-independent and “antisymmetric” spin-dependent interaction terms are given by  $\lambda_s = \frac{2}{3}(a_0 + 2a_2)/a_{\perp}$  and  $\lambda_a = \frac{2}{3}(a_2 - a_0)/a_{\perp}$ , respectively, where  $a_0$  and  $a_2$  correspond to the  $s$ -wave scattering lengths of two atoms in the scattering channels with total spin  $F = 0$  and  $F = 2$ , and  $a_{\perp} = \sqrt{\hbar/(M\omega_{\perp})}$ , with  $M$  being the atomic mass of Rb. In our case,  $\lambda_s \approx 5.2 \times 10^{-3}$  and  $\lambda_a \approx -2.4 \times 10^{-5}$ ; i.e.,  $\lambda_a/|\lambda_s|$  is a small parameter.

Based on this fact, it can readily be observed that—in the absence of the trap, and ignoring the spin-dependent

interactions—the GPEs (1a)–(1b) reduce to the completely integrable Manakov system [52]. This model admits vector soliton solutions of the mixed type (i.e., DB soliton complexes; cf., e.g., Ref. [53]) which may persist in the presence of the spin-dependent terms of Eqs. (1a)–(1b) and the trap. To make our point stronger, and to better understand the role of the spin-dependent nonlinear interatomic interactions, we exploit the smallness of  $\lambda_a/|\lambda_s|$  and employ (for  $V(x) = 0$ ) a multiscale expansion method to find approximate soliton solutions of Eqs. (1a)–(1b). Here, instead of using a single-mode approximation [51,54] for the symmetric states  $|1, -1\rangle$  and  $|1, +1\rangle$  as in Ref. [39], we impose nontrivial boundary conditions for the  $|1, -1\rangle$  component and trivial ones for the  $|1, 0\rangle$  and  $|1, +1\rangle$  components, to derive DBB soliton solutions for sublevels  $m_F = -1, 0, +1$ , respectively. We can thus show (see Supplemental Material [55] for details, which includes Refs. [56–59]) that the wave functions of DBB solitons take the following form:

$$\begin{aligned}\psi_{-1} &\approx \sqrt{n_0 + \epsilon n(X, T)} e^{-i\mu_{-1}t + i\epsilon^{1/2}C^{-1}(\lambda_s + \lambda_a)} \int n dX, \\ \psi_{0,+1} &\approx \epsilon^{3/4} q_{0,+1}(X, T) e^{i[Cx - (\frac{1}{2}C^2 + \mu_{0,+1})t]},\end{aligned}\quad (2)$$

where  $\epsilon$  is a formal small parameter,  $\mu_{\mp 1} = (\lambda_s \pm \lambda_a)n_0$  and  $\mu_0 = \lambda_s n_0$  are the chemical potentials of the three components, while  $n_0$  and  $C^2 = \mu_{-1}$  denote, respectively, the steady-state density and the (squared) speed of sound of the  $|1, -1\rangle$  component. Finally, the functions  $n(X, T)$  and  $q_{0,+1}(X, T)$ , which depend on the stretched variables  $X = \epsilon^{1/2}(x - Ct)$  and  $T = \epsilon t$ , obey the system:

$$\begin{aligned}\partial_T n &= -\sqrt{\mu_{-1}} \partial_X (|q_0|^2) - \frac{\mu_{+1}}{\sqrt{\mu_{-1}}} \partial_X (|q_{+1}|^2), \\ i\partial_T q_0 + \frac{1}{2} \partial_X^2 q_0 - \frac{\mu_0}{n_0} n q_0 &= 0, \\ i\partial_T q_{+1} + \frac{1}{2} \partial_X^2 q_{+1} - \frac{\mu_{+1}}{n_0} n q_{+1} &= 0.\end{aligned}\quad (3)$$

The above system, which long-short wave resonant interaction (LSRI) [44], is the multicomponent generalization of the so-called Yajima-Oikawa (YO) system, originally derived to describe the interaction of Langmuir and sound waves in plasmas [41]. In fact, Eqs. (3) constitute the so-called multicomponent YO (mYO) system, originally introduced in the context of many-component magnon-phonon systems [42], which generalizes the YO model [43]. This model has recently attracted considerable attention due to its variety of solutions and interesting soliton collision properties [60–62]. Similarly to the single-component YO model, the mYO system is completely integrable, and possesses soliton solutions of the form [60]  $n \propto -\text{sech}^2(K_s X - \Omega_s T)$  and  $q_{0,+1} \propto \text{sech}(K_s X - \Omega_s T)$ , where  $K_s$  and  $\Omega_s$  are constants. When substituted into Eqs. (2), these expressions give rise to approximate DBB

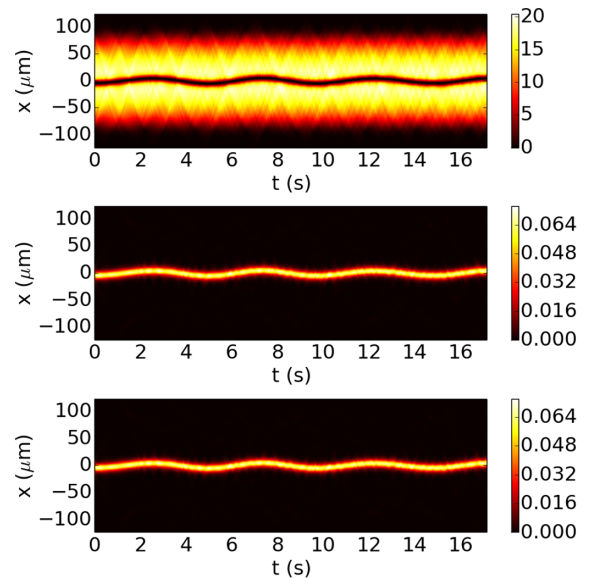


FIG. 2. Top panel: Numerical simulation of the evolution of the densities  $|\psi_{-1}|^2$  (top),  $|\psi_0|^2$  (middle), and  $|\psi_{+1}|^2$  (bottom) as per Eqs. (1a)–(1b) in the case where a small spatial displacement of the DBB structure is initiated at  $t = 0$ . It is observed that robust oscillations of the DBB structure persist for several seconds.

solitons, for the  $m_F = -1, 0, +1$  spin components, respectively.

Direct numerical simulations corroborate our experimental and analytical findings. In the performed simulations, the total number of atoms and energy of the system (cf., e.g., Ref. [51] for definitions) are conserved up to a negligible error. First, we have found (results not shown here) that the above-mentioned small-amplitude solitons persist for large amplitudes. Second, apart from the traveling DBB solitons, we were also able to identify robust stationary such structures in the presence of the trap. A solution is constructed by identifying, at first, a stationary DB soliton state of the form  $\psi_{-1}(x, 0) = \sqrt{\lambda_s^{-1}[\mu_{-1} - V(x)]} \tanh(\sqrt{\mu_{-1}}x)$ ,  $\psi_0(x, 0) = \text{Asech}(\sqrt{\mu_0}x)$  and  $\psi_{+1}(x, 0) = 0$ . Then, in line with our experimental protocol, switching on a Rabi coupling between components  $|1, 0\rangle$  and  $|1, +1\rangle$  for a finite time interval, atoms are transferred to  $\psi_{+1}$  and a bright soliton is formed there too. After switching off the Rabi coupling between  $\psi_0$  and  $\psi_{+1}$ , the percentage population of atoms in the three components is 97:2:1. We have also performed numerical simulations for the DBB solitons in the presence of a trap, in the case where the soliton is displaced from the trap center. We have confirmed in such a case that the DBB solitons generically perform robust oscillations inside the trap. A typical example is shown in Fig. 2 illustrating that—despite the potential presence of sound waves inside the condensate—the oscillation persists for very long times of the order of many seconds. In this setting, we have also developed an approximate characterization of the oscillation frequency  $\omega$  of the DBB solitons given by

$$\omega^2 = \frac{\Omega^2}{2} \left( 1 - \frac{N_b}{4\sqrt{\mu + (\frac{N_b}{4})^2}} \right), \quad (4)$$

for chemical potential  $\mu$  of the dark component, and total atomic population for the bright components equal to  $N_b = N_{b,1} + N_{b,2}$  (where subscripts 1 and 2 denote the bright soliton components) confined by a parabolic trap of strength  $\Omega$ . The detailed explanation of this result, stemming from the work of Ref. [63] for DB solitons (see also Ref. [64] for dark solitons), is provided in the Supplemental Material [55]; there, the result (4) is also systematically corroborated by means of direct numerical simulations, showing that it is always within 7.5% of numerically identified DBB oscillation frequency.

Oscillatory motion of DBB solitons is also observed in our experiments. For typical parameters, the experimentally observed periods are on the order of many seconds, on the same order of magnitude as seen, e.g., in the numerical results of Fig. 2. Preliminary experimental results are presented in Fig. 1(c). A precision study, however, requires addressing numerous technical issues (including, e.g., the slow decay in atom numbers over the course of the oscillation and the variability of the exact starting conditions) and is, thus, beyond the scope of the current Letter.

Apart from DBB solitons, in our experiments we have also observed the emergence of DDB ones, again with lifetimes on the order of hundreds of milliseconds. To generate DDB solitons, a procedure similar to that of the DBB soliton generation is followed. We begin with all atoms in the  $|1, 0\rangle$  state. A small fraction of atoms is then uniformly transferred from the  $|1, 0\rangle$  state to the  $|1, +1\rangle$  state. Subsequently, a weak magnetic gradient is applied and leads to the formation of DB solitons. In this experiment, the dark solitons reside in the  $|1, 0\rangle$  state, while the bright soliton components are formed by atoms in the  $|1, +1\rangle$  state. After the DB solitons are formed, the magnetic gradient is removed, which is necessary to ensure long lifetimes of the solitonic structures. To convert the DB solitons into DDB ones, a rf sweep is used to transfer an adjustable fraction of the atoms from the  $|1, 0\rangle$  state to the  $|1, -1\rangle$  state. This completes the formation of a DDB soliton.

The existence of these features appears to be fairly insensitive to the exact population ratio of the three Zeeman states. For example, we have experimentally verified the existence of DDB structures for different percentage population of atoms in the three states including 71:21:8, 53:38:9, and 33:66:1. These results highlight the generic robustness of the DDB structures. A pertinent example is shown in Fig. 3.

The formation of DDB solitons can also be predicted in the framework of the multiscale expansion method [55]. In this case, assuming approximately equal chemical potential for all spin components,  $\mu \approx \lambda_s(1 + r^2)$  (where

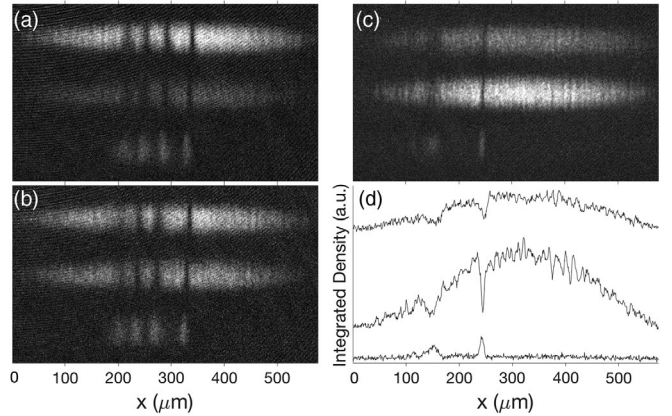


FIG. 3. (a)–(c) Experimental TOF images of DDB solitons. Here it is shown that the DDB solitons can be generated for a large variation of the total relative populations of the  $|1, -1\rangle$ ,  $|1, 0\rangle$ , and  $|1, +1\rangle$  states (upper, middle, and lower cloud in each image, respectively). In each case, to verify the stability of the soliton a 100 ms in-trap evolution time is applied after DDB soliton formation. The relative populations of the three states are (a) 71:21:8, (b) 53:38:9, and (c) 33:66:1. (d) Integrated density profiles of the Zeeman levels of image (c). The plots are offset in the y dimension for clarity and to mimic the spatial order of each state in the TOF image.

$n_0$  is the pertinent steady-state density and  $r = |\psi_0|/|\psi_{-1}|$ , we can show that DDB solitons do exist, and assume the following form:

$$\begin{aligned} \psi_{-1} &\approx \sqrt{n_0 + \epsilon \rho(X, T)} e^{-i\mu t + i\epsilon^{1/2}\sqrt{\mu} \int \rho(X, T) dX}, \\ \psi_0 &= r\psi_{-1}, \quad \psi_{+1} \approx \epsilon^{3/4} q(X, T) e^{i[\sqrt{\mu}x - (3/2)\mu t]}, \end{aligned} \quad (5)$$

where  $\epsilon$  is again a small parameter,  $X = \epsilon^{1/2}(x - \sqrt{\mu}t)$  and  $T = \epsilon t$  are stretched variables, and the functions  $\rho(X, T)$  and  $q(X, T)$  are governed by the equations:

$$\begin{aligned} \partial_T \rho &= -\sqrt{\mu}(\lambda_s + \lambda_a) \partial_X (|q|^2), \\ i\partial_T q + \frac{1}{2} \partial_X^2 q - (\mu/n_0)\rho q &= 0. \end{aligned} \quad (6)$$

The above equations constitute the single component Yajima-Oikawa (YO) system [41]. The YO system is completely integrable and possesses soliton solutions of the form  $\rho \propto -\text{sech}^2(k_s X - \omega_s T)$  and  $q \propto \text{sech}(k_s X - \omega_s T)$ , where  $k_s$  and  $\omega_s$  are constants. These expressions, when substituted into Eqs. (5), give rise to approximate DDB solitons, for the  $m_F = -1, 0, +1$  spin components, respectively. Note that we have found (results not shown here) that such DDB solitons are also long-lived in our direct numerical simulations.

In conclusion, we have demonstrated the creation of DBB and DDB solitons in an  $F = 1$   $^{87}\text{Rb}$  condensate. It was found that these structures are quite robust, featuring lifetimes on the order of several hundreds of milliseconds,

and can be formed for different relative populations of atoms in the three Zeeman states. We have employed a perturbative approach to show that these mixed solitons can be approximated by solutions of the multi- and single-component Yajima-Oikawa systems. This connection also underscores the breadth of relevance of these patterns and supports their robustness. Direct numerical simulations corroborate our results, indicating that these solitons can persist but also that they can robustly oscillate in the condensates.

The experimental, theoretical, and numerical manifestation of such states paves the way for a number of interesting studies in the future. For instance, it will be particularly relevant to explore more systematically the dynamics and interactions of the DBB and DDB solitons in quasi-one-dimensional settings, comparing them with their integrable Yajima-Oikawa counterparts [60–62]. Another possibility is to study generalizations of such spinorial states in higher dimensions, constructing spinorial vortex-bright (or baby-Skyrmion, or filled-core vortex) states [4] to understand their dynamics and interactions. Soliton interaction dynamics and stability over parametric variations (e.g., of the spin-dependent part of the Hamiltonian) would also be particularly relevant to consider even in the one-dimensional case. More broadly, spinor BECs open an avenue to proceed beyond two-component soliton dynamics that may yield exciting developments in the near future.

This material is based upon work supported by the National Science Foundation under Grants No. PHY-1607495 (P. E.) and No. PHY-1602994 (P. G. K.).

- [10] A. L. Marchant, T. P. Billam, T. P. Wiles, M. M. H. Yu, S. A. Gardiner, and L. Cornish, *Nat. Commun.* **4**, 1865 (2013).
- [11] J. H. V. Nguyen, D. Luo, and R. G. Hulet, *Science* **356**, 422 (2017).
- [12] S. Burger, K. Bongs, S. Dettmer, W. Ertmer, K. Sengstock, A. Sanpera, G. V. Shlyapnikov, and M. Lewenstein, *Phys. Rev. Lett.* **83**, 5198 (1999).
- [13] J. Denschlag, J. E. Simsarian, D. L. Feder, C. W. Clark, L. A. Collins, J. Cubizolles, L. Deng, E. W. Hagley, K. Helmerson, W. P. Reinhardt, S. L. Rolston, B. I. Schneider, and W. D. Phillips, *Science* **287**, 97 (2000).
- [14] Z. Dutton, M. Budde, C. Sloane, and L. V. Hau, *Science* **293**, 663 (2001).
- [15] B. P. Anderson, P. C. Haljan, C. A. Regal, D. L. Feder, L. A. Collins, C. W. Clark, and E. A. Cornell, *Phys. Rev. Lett.* **86**, 2926 (2001).
- [16] C. Becker, S. Stellmer, P. Soltan-Panahi, S. Dörscher, M. Baumert, E.-M. Richter, J. Kronjäger, K. Bongs, and K. Sengstock, *Nat. Phys.* **4**, 496 (2008).
- [17] S. Stellmer, C. Becker, P. Soltan-Panahi, E.-M. Richter, S. Dörscher, M. Baumert, J. Kronjäger, K. Bongs, and K. Sengstock, *Phys. Rev. Lett.* **101**, 120406 (2008).
- [18] I. Shomroni, E. Lahoud, S. Levy, and J. Steinhauer, *Nat. Phys.* **5**, 193 (2009).
- [19] A. Weller, J. P. Ronzheimer, C. Gross, J. Esteve, M. K. Oberthaler, D. J. Frantzeskakis, G. Theocharis, and P. G. Kevrekidis, *Phys. Rev. Lett.* **101**, 130401 (2008).
- [20] G. Theocharis, A. Weller, J. P. Ronzheimer, C. Gross, M. K. Oberthaler, P. G. Kevrekidis, and D. J. Frantzeskakis, *Phys. Rev. A* **81**, 063604 (2010).
- [21] P. Engels and C. Atherton, *Phys. Rev. Lett.* **99**, 160405 (2007).
- [22] D. S. Hall, M. R. Matthews, J. R. Ensher, C. E. Wieman, and E. A. Cornell, *Phys. Rev. Lett.* **81**, 1539 (1998).
- [23] D. M. Stamper-Kurn, M. R. Andrews, A. P. Chikkatur, S. Inouye, H.-J. Miesner, J. Stenger, and W. Ketterle, *Phys. Rev. Lett.* **80**, 2027 (1998).
- [24] C. Hamner, J. J. Chang, P. Engels, and M. A. Hoefer, *Phys. Rev. Lett.* **106**, 065302 (2011).
- [25] S. Middelkamp, J. J. Chang, C. Hamner, R. Carretero-González, P. G. Kevrekidis, V. Achilleos, D. J. Frantzeskakis, P. Schmelcher, and P. Engels, *Phys. Lett. A* **375**, 642 (2011).
- [26] D. Yan, J. J. Chang, C. Hamner, P. G. Kevrekidis, P. Engels, V. Achilleos, D. J. Frantzeskakis, R. Carretero-González, and P. Schmelcher, *Phys. Rev. A* **84**, 053630 (2011).
- [27] A. Álvarez, J. Cuevas, F. R. Romero, C. Hamner, J. J. Chang, P. Engels, P. G. Kevrekidis, and D. J. Frantzeskakis, *J. Phys. B* **46**, 065302 (2013).
- [28] M. A. Hoefer, J. J. Chang, C. Hamner, and P. Engels, *Phys. Rev. A* **84**, 041605(R) (2011).
- [29] D. Yan, J. J. Chang, C. Hamner, M. Hoefer, P. G. Kevrekidis, P. Engels, V. Achilleos, D. J. Frantzeskakis, and J. Cuevas, *J. Phys. B* **45**, 115301 (2012).
- [30] I. Danaila, M. A. Khamehchi, V. Gokhroo, P. Engels, and P. G. Kevrekidis, *Phys. Rev. A* **94**, 053617 (2016).
- [31] P. G. Kevrekidis and D. J. Frantzeskakis, *Rev. Phys.* **1**, 140 (2016).
- [32] Z. Chen, M. Segev, T. H. Coskun, D. N. Christodoulides, and Yu. S. Kivshar, *J. Opt. Soc. Am. B* **14**, 3066 (1997).

[33] E. A. Ostrovskaya, Yu. S. Kivshar, Z. Chen, and M. Segev, *Opt. Lett.* **24**, 327 (1999).

[34] Yu. S. Kivshar and G. P. Agrawal, *Optical Solitons: From Fibers to Photonic Crystals* (Academic Press, San Diego, 2003).

[35] B. Luther-Davies and X. Yang, *Opt. Lett.* **17**, 496 (1992).

[36] J. Stenger, S. Inouye, D. M. Stamper-Kurn, H.-J. Miesner, A. P. Chikkatur, and W. Ketterle, *Nature (London)* **396**, 345 (1998).

[37] Y. Kawaguchi and M. Ueda, *Phys. Rep.* **520**, 253 (2012).

[38] D. M. Stamper-Kurn and M. Ueda, *Rev. Mod. Phys.* **85**, 1191 (2013).

[39] H. E. Nistazakis, D. J. Frantzeskakis, P. G. Kevrekidis, B. A. Malomed, and R. Carretero-González, *Phys. Rev. A* **77**, 033612 (2008).

[40] B. Xiong and J. Gong, *Phys. Rev. A* **81**, 033618 (2010).

[41] N. Yajima and M. Oikawa, *Prog. Theor. Phys.* **56**, 1719 (1976).

[42] R. Myrzakulov, O. K. Pashaev, and Kh. T. Kholmurodov, *Phys. Scr.* **33**, 378 (1986).

[43] Y. Ohta, K. Maruno, and M. Oikawa, *J. Phys. A* **40**, 7659 (2007).

[44] V. E. Zakharov, *Sov. Phys. JETP* **35**, 908 (1972).

[45] D. J. Benney, *Stud. Appl. Math.* **56**, 81 (1977).

[46] Yu. S. Kivshar, *Opt. Lett.* **17**, 1322 (1992).

[47] A. Chowdhury and J. A. Tataronis, *Phys. Rev. Lett.* **100**, 153905 (2008).

[48] R. S. Tasgal and Y. B. Band, *Phys. Rev. A* **87**, 023626 (2013); **91**, 013615 (2015).

[49] For imaging, the trap is suddenly switched off and a vertical magnetic gradient is applied. Because of this gradient, the three Zeeman states are separated along the vertical z direction after a brief time of flight (13 ms). An image is then taken along the y direction, showing the position of the three atom clouds.

[50] J.-P. Martikainen, A. Collin, and K.-A. Suominen, *Phys. Rev. A* **66**, 053604 (2002).

[51] B. J. Dabrowska-Wüster, E. A. Ostrovskaya, T. J. Alexander, and Yu. S. Kivshar, *Phys. Rev. A* **75**, 023617 (2007).

[52] S. V. Manakov, *Sov. Phys. JETP* **38**, 248 (1974).

[53] B. F. Feng, *J. Phys. A* **47**, 355203 (2014).

[54] H. Pu, C. K. Law, S. Raghavan, J. H. Eberly, and N. P. Bigelow, *Phys. Rev. A* **60**, 1463 (1999).

[55] See Supplemental Material at <http://link.aps.org/supplemental/10.1103/PhysRevLett.120.063202> for the derivation of the Yajima-Oikawa systems and the DBB and DDB soliton solutions, as well as for the oscillation frequency of DBB solitons.

[56] P. B. Lundquist, D. R. Andersen, and Yu. S. Kivshar, *Phys. Rev. E* **57**, 3551 (1998).

[57] V. E. Zakharov and L. A. Ostrovsky, *Physica (Amsterdam)* **238D**, 540 (2009).

[58] M. J. Ablowitz, *Nonlinear Dispersive Waves: Asymptotic Analysis and Solitons* (Cambridge University Press, Cambridge, England, 2011).

[59] R. K. Dodd, J. C. Eilbeck, J. D. Gibbon, and H. C. Morris, *Solitons and Nonlinear Wave Equations* (Academic, New York, 1984).

[60] T. Kanna, K. Sakkaravarthi, and K. Tamilselvan, *Phys. Rev. E* **88**, 062921 (2013).

[61] K. Sakkaravarthi, T. Kanna, M. Vijayajayanthi, and M. Lakshmanan, *Phys. Rev. E* **90**, 052912 (2014); T. Kanna, M. Vijayajayanthi, and M. Lakshmanan, *Phys. Rev. E* **90**, 042901 (2014).

[62] J. Chen, Y. Chen, B. F. Feng, and K. Maruno, *J. Phys. Soc. Jpn.* **84**, 074001 (2015); **84**, 034002 (2015).

[63] Th. Busch and J. R. Anglin, *Phys. Rev. Lett.* **87**, 010401 (2001).

[64] Th. Busch and J. R. Anglin, *Phys. Rev. Lett.* **84**, 2298 (2000).